Determining Exchange Splitting in a Magnetic Semiconductor by Spin-Filter Tunneling

T. S. Santos,[1,*] J. S. Moodera,[1] K. V. Raman,[1] E. Negusse,[2] J. Holroyd,[2] J. Dvorak,[2] M. Liberati,[2] Y. U. Idzerda,[2] and E. Arenholz[3]

[1]Francis Bitter Magnet Laboratory, Massachusetts Institute of Technology, Cambridge, Massachusetts 02139, USA
[2]Department of Physics, Montana State University, Bozeman, Montana 59717, USA
[3]Advanced Light Source, Lawrence Berkeley National Laboratory, Berkeley, California 94720, USA

(Received 24 June 2008; published 30 September 2008)

A large exchange splitting of the conduction band in ultrathin films of the ferromagnetic semiconductor EuO was determined quantitatively, by using EuO as a tunnel barrier and fitting the current-voltage characteristics and temperature dependence to tunneling theory. This exchange splitting leads to different tunnel barrier heights for spin-up and spin-down electrons and is large enough to produce a near-fully spin-polarized current. Moreover, the magnetic properties of these ultrathin films (<6 nm) show a reduction in Curie temperature with decreasing thickness, in agreement with theoretical calculation [R. Schiller *et al.*, Phys. Rev. Lett. **86**, 3847 (2001)].

DOI: 10.1103/PhysRevLett.101.147201 PACS numbers: 75.70.Ak, 72.25.Hg, 73.43.Jn, 75.50.Pp

Ferromagnetic semiconductors (FSs) having a tunable charge carrier concentration that is spin-polarized are ideally suited as spin injectors and detectors in semiconductor spintronic devices. The europium chalcogenides stand out among the FSs as ideal Heisenberg ferromagnets, with a high magnetic moment and a large exchange splitting of the conduction band [1]. Utilizing the exchange splitting ($2\Delta E_{ex}$) to filter spins, these materials produce a near-fully spin-polarized current when used as a tunnel barrier [2–4], making them strong candidates for spin injection in semiconductors. Of the Eu chalcogenides, EuO has the largest $2\Delta E_{ex}$ and the highest Curie temperature ($T_C = 69$ K for bulk). However, due to the high reactivity of EuO with air, preparation of thin films of EuO is highly challenging, precluding the study of EuO down to a few monolayers. Successful preparation of chemically stable, high-quality EuO as tunnel barriers in this work has allowed for the study of EuO at the ultrathin thickness scale, illuminating its magnetic properties, exchange splitting, and spin-filter capability at the few-monolayers range.

In EuO, the large saturation magnetic moment $\mu g J = 7\mu_B$ per Eu^{2+} originates from the seven unpaired electrons localized at the $4f$ levels in the energy gap between the valence band and the conduction band, shown schematically in Fig. 1. The optical band gap ($E_g = 1.1$ eV) is the energy gap between the $4f$ levels and the conduction band. Ferromagnetic order of the $4f$ spins causes Zeeman splitting of the conduction band, lowering (raising) the spin-up (-down) band symmetrically by ΔE_{ex}. Thus, free carriers in the conduction band are spin-polarized. A large exchange splitting of 0.54 eV was first determined by measuring the redshift of the absorption edge in single crystals of EuO cooled below T_C [1,5].

When an ultrathin film of EuO is used as the tunnel barrier between two metallic electrodes, the exchange splitting of the conduction band gives rise to a lower barrier height for spin-up electrons $\Phi_\uparrow$ $(=\Phi_0 - \Delta E_{ex})$ and a higher barrier height for spin-down electrons $\Phi_\downarrow$ $(=\Phi_0 + \Delta E_{ex})$, where Φ_0 is the barrier height at $T > T_C$. Because the tunnel current depends exponentially on the barrier height [6], the tunneling probability for spin-up electrons is much greater than for spin-down electrons, leading to a highly spin-polarized current—a phenomenon called the spin-filter effect [7]. Using a spin-filter tunnel barrier, as opposed to a ferromagnetic metal, is a unique approach to achieving a spin-polarized current with built-in advantages, such as interfacial band matching and a sharper interface.

Because the splitting in bulk EuO is significant compared to E_g, EuO could potentially produce total spin polarization ($P = 100\%$). However, only a few monolayers of EuO are needed for tunneling, which can be expected to have different properties than bulk. For example, Schiller *et al.* [8] calculated the electronic structure and magnetic properties of ultrathin, single-crystal EuO (100) and found a reduction in T_C from the bulk value as the thickness approached a few monolayers. However, due

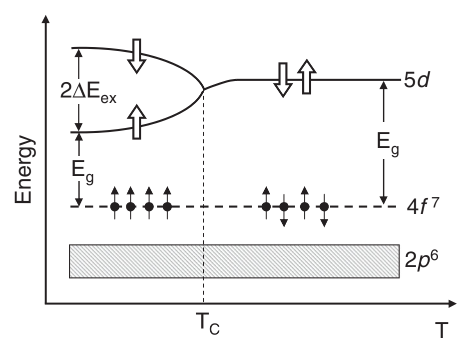

FIG. 1. Schematic of the energy gap of EuO, showing the exchange splitting in the $5d$ conduction band for $T < T_C$, lowering the spin-up sublevel from the spin-down sublevel by $2\Delta E_{ex}$. This figure was modified from Ref. [1].

to the difficulty in preparing ultrathin EuO films, their calculation had not been experimentally verified. Furthermore, a reduction in T_C for ultrathin EuO raises the question as to whether a reduction in $2\Delta E_{\mathrm{ex}}$ should be expected as well, which is directly relevant to spin filtering.

In this study using well-characterized, high-quality, ultrathin EuO films, we investigated this Heisenberg ferromagnet in the few-monolayers regime, allowing us to verify the model by Schiller *et al.* In addition, by detailed transport measurements of tunnel junctions with EuO barriers, we uniquely determined the amount of exchange splitting for ultrathin EuO.

Films of EuO were made by thermal reactive deposition, whereby pure europium metal was evaporated in the presence of a dynamic oxygen partial pressure of 3×10^{-7} Torr. Eu_2O_3, with a heat of formation $\Delta H_f = -1730$ kJ/mol compared to -608 kJ/mol for EuO [9], forms more readily. Because Eu_2O_3 is paramagnetic, and thus not a spin filter, the Eu metal evaporation rate and oxygen flow were carefully controlled in order to produce optimum EuO. To study the dependence of T_C on film thickness, a wedge film was made in opening-shutter mode with thickness ranging from 1 to 6 nm, in steps of 1 nm. The magnetic and chemical properties of the films were found to be critically dependent upon the materials selection for the top and bottom interface layers [4,10]. The wedge was deposited onto a Si/50 nm SiO_2 substrate with a Cu bottom layer and a Y capping layer. Films prepared under these conditions are known to be polycrystalline [4]. The films were characterized by superconducting quantum interference device (SQUID) magnetometry, x-ray absorption spectroscopy (XAS), and x-ray magnetic circular dichroism (XMCD). Tunnel junctions were patterned *in situ* using shadow masks, forming a cross configuration with a junction area of (200×200) $\mu\mathrm{m}^2$. Deposition rate and thickness were determined *in situ* by a quartz crystal monitor. Given that the crystal is located at a distance from the substrate and the oxygen inlet, the actual thickness may be greater than the nominal thickness to within 15%.

Figure 2 displays magnetization (M) versus temperature (T) for 1–6 nm EuO films, showing a clear trend toward lower T_C as film thickness decreases. The T_C of the thicker films approach that of bulk, while the thinnest, 1 nm film has a T_C of 30 K. This is the general behavior of ferromagnetic films and is also what is predicted by Schiller *et al.* This trend is caused by the lower coordination of the Eu^{2+} ions at the interfaces, such that the increasing, atomic surface-to-volume ratio for the thinner films leads to weaker exchange interactions. Experimental data are compared with the calculation of Schiller *et al.* in the inset in Fig. 2. Overall, the experimental values are lower than the theoretical curve. This is not unreasonable when consider-

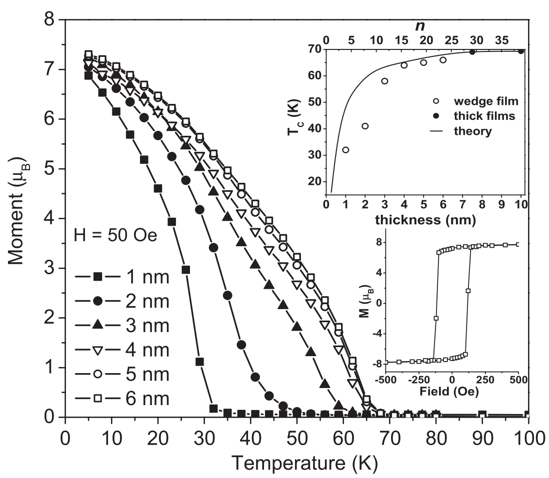

FIG. 2. Dependence of T_C on thickness of EuO film with the structure: 2 nm Cr/9 nm Cu/EuO/2 nm Y/8 nm Al. Top inset: T_C dependence compared with Schiller *et al.* [8], where n is the number of monolayers. The T_C of thicker EuO films made separately are also plotted for reference. Bottom inset: Hysteresis loop of the 6 nm film at 5 K. The measured moment $>7\mu_B$ is likely due to an underestimation of film thickness, as described in text.

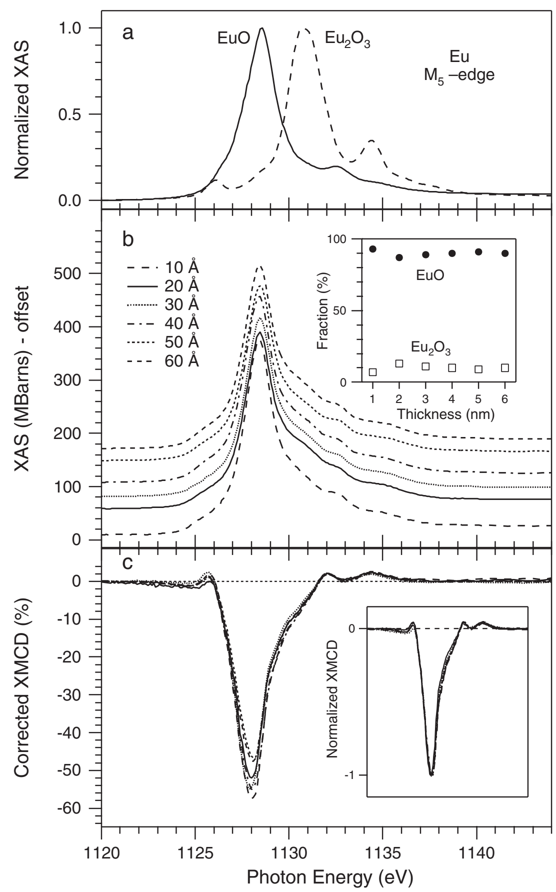

FIG. 3. (a) Normalized reference XAS spectra at the M_5 edge for EuO and Eu_2O_3 films. (b) XAS of the 1–6 nm EuO wedge (same as in Fig. 2) at 295 K. Inset: Relative amounts of EuO and Eu_2O_3 computed by deconvolving the XAS spectra. (c) Corrected XMCD spectra; corrections as described in text. Inset: Normalized MCD spectra.

ing that the calculation was done for free-floating, single-crystal EuO, whereas the films in this experiment are polycrystalline, with materials at the interfaces. The moment at 5 K closely matches the bulk value of $7\mu_B$.

The chemical composition and magnetic properties of these ultrathin EuO films were further investigated using XAS and XMCD. At the europium $3d_{5/2}$ (M_5) absorption edge, Eu^{2+} and Eu^{3+} have distinct signature peaks, as shown in Fig. 3(a) for reference films of EuO and Eu_2O_3 [11–13]. For all film thicknesses, the Eu^{2+} peak is clearly dominant, as shown in Fig. 3(b). In order to obtain the relative amounts of EuO and Eu_2O_3, shown in the inset in Fig. 3(b), the XAS spectra were deconvolved against the reference EuO and Eu_2O_3 spectra, resulting in ~90% EuO for all film thicknesses.

The XMCD, measured at 18 K with 90% circularly polarized light at a 60° incidence angle in the presence of a ± 0.5 T magnetic field, is presented in Fig. 3(c) as the difference in the XAS spectra for parallel and antiparallel alignment of photon polarization and magnetization direction, respectively. The displayed XMCD are corrected for the fraction of Eu^{2+}, incomplete light polarization, incidence angle, and finite temperature reduction of the moment (i.e., the spectra would be observed for pure EuO that is fully magnetized with 100% circularly polarized light at grazing incidence and at $T = 0$ K) [14]. After the corrections, the maximum XMCD signal is measured to be $52.0\% \pm 4.3\%$. This XMCD value is in excellent agreement with the theoretically expected value of 51% for EuO [11,13]. Additionally, the Eu^{2+} XAS and XMCD spectra are identical to the Gd^{3+} spectra for GdN as measured by Leuenberger *et al.* [15], as was theoretically proposed [11]. For comparison, the normalized XMCD spectra for all thicknesses are shown in the inset in Fig. 3(c), confirming that the dichroism, and hence the magnetization, originates entirely from EuO, as expected. These XAS and XMCD measurements, along with the SQUID measurements, show the excellent quality of these ultrathin EuO films.

Next, we address the transport behavior. The junction resistance (R_J) of tunnel junctions with the structure 3.6 nm Al/0.4 nm Mg/2.5 nm EuO/4.0 nm Y/8.0 nm Al [16] was measured as a function of T, using a 4-point configuration with a constant bias applied with respect to the Y electrode. As T decreased below room temperature, R_J increased as is common for a semiconducting barrier, whereas at low temperatures R_J *decreased*. As shown in Fig. 4(a), when the junction was cooled below the T_C of EuO, R_J decreased dramatically. This is due to the lowering of the spin-up barrier height caused by the exchange splitting in EuO (see Fig. 1). The drop in R_J is large, as much as 2 orders of magnitude for these junctions, showing substantial exchange splitting. Such a resistance drop was consistently observed for all junctions. This is in contrast to the typical $R_J(T)$ behavior for a nonmagnetic barrier, such as Al_2O_3, for which Φ is constant at all T and R_J increases monotonically by ~15% as T decreases [17].

The exchange splitting in this 2.5 nm EuO barrier is quantitatively determined from $R_J(T)$ and current-voltage (I-V) measurements in the following way. First, by fitting the I-V curve to the Brinkman-Dynes-Rowell (BDR) model [6] for tunneling between two metals through an insulating barrier, the average barrier height Φ_0 and thickness d were found. Beginning with the I-V curve at 98 K, at which $2\Delta E_{ex} = 0$, the BDR fit yielded $\Phi_0 = 0.92 \pm 0.01$ eV and $d = 3.1 \pm 0.1$ nm. Then, holding the Φ_0 and d values constant, the I-V curve at 6 K was fit by varying ΔE_{ex} such that $\Phi_0 - \Delta E_{ex} = \Phi_\uparrow$ and $\Phi_0 + \Delta E_{ex} = \Phi_\downarrow$, and the total current $I = I_\uparrow + I_\downarrow$, where the spin-up (spin-down) current $I_\uparrow$ ($I_\downarrow$) corresponds to $\Phi_\uparrow$ ($\Phi_\downarrow$). This procedure yielded $2\Delta E_{ex} = 0.29 \pm 0.01$ eV, which is quite large for this ultrathin EuO film, though reduced from the bulk value of 0.54 eV. Importantly, it is seen here that tunneling can be utilized to quantitatively determine the exchange splitting in a magnetic insulator, the first such demonstration of extending the principle of electron tunneling to study magnetism in ultrathin films, which is nontrivial, especially in systems as unstable as EuO.

Data analysis using the BDR model was performed for I-V curves in the bias range -150 to 150 mV, which is consistent with the $R_J(T)$ curve at $V = 100$ mV, plotted in Fig. 4(b). Limiting the fit to this range ensured that Φ_0 was

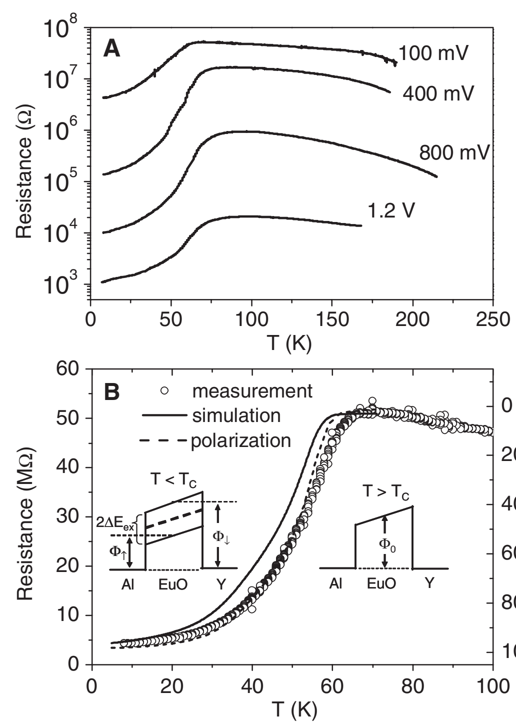

FIG. 4. (a) $R_J(T)$ for a Al/EuO/Y junction, measured at the biases indicated, shows the reduction in R_J for $T < T_C$ due to exchange splitting in the EuO barrier. (b) $R_J(T)$ measured with 100 mV, replotted from (a). $R_J(T)$ was simulated using the $M(T)$ behavior for the 3 nm film from Fig. 2 and assuming that $M(T) \propto 2\Delta E_{ex}(T)$. Zero P was deduced for $T > T_C$, and P increased as splitting increased for $T < T_C$, reaching 98%. Inset: Energy barrier profile for $T < T_C$ and $T > T_C$.

not a function of bias [6,18]. Shown along with the measured $R_J(T)$ is a simulated $R_J(T)$ curve obtained by calculating R_J using the BDR relation, with $\Phi_0 = 0.92$ eV and $d = 3.1$ nm, and from the $M(T)$ curve in Fig. 2 for the 3 nm EuO film. Here the assumption was that $2\Delta E_{ex}$ varies with temperature as $M(T)$, such that $\frac{2\Delta E_{ex}(T)}{2\Delta E_{ex}(T=5\ \mathrm{K})} = \frac{M(T)}{M(T=5\ \mathrm{K})}$. The good agreement between the measurement and the simulation nicely correlates the transport in the EuO barrier to its magnetization.

Furthermore, knowing the $I_\uparrow$ and $I_\downarrow$ values from the BDR fit, the spin polarization of the tunnel current is calculated from $P = (I_\uparrow - I_\downarrow)/(I_\uparrow + I_\downarrow)$, shown in Fig. 4(b). This resulted in nearly total polarization of 98% for $2\Delta E_{ex} = 0.29$ eV ($P = 0$ for $2\Delta E_{ex} = 0$). Thus, the splitting in this ultrathin EuO barrier is large enough to produce a near-fully spin-polarized current, demonstrating its potential as an ideal spin source. The same analysis carried out on tunneling measurements for a 1.5 nm EuO barrier from the same sample set yielded $\Phi_0 = 0.35$ eV, $2\Delta E_{ex} = 0.10$ eV, and $P = 97\%$. Despite the smaller $2\Delta E_{ex}$ for the thinner barrier, in line with the lower T_C, a large P is still produced because the splitting remains substantial relative to the lower average barrier height of the thinner barrier.

It should be noted that this analysis does not take into account any spin scattering events that could cause a loss of P during tunneling, such as interfacial impurities, defect states, or excitation of magnons at high bias. A spin detector, such as a superconducting electrode used in the Meservey-Tedrow technique [19], or a ferromagnetic electrode used in a quasimagnetic tunnel junction structure [7,20], would directly probe P.

Figure 4(a) also shows $R_J(T)$ at higher applied bias. The amount of decrease in R_J [given by $\frac{\Delta R}{R} = \frac{R_{J,\max} - R_J(6\ \mathrm{K})}{R_{J,\max}}$, where $R_{J,\max}$ is the maximum R_J] is larger at 400 and 800 mV. High bias can drastically deform the potential barrier, resulting in Fowler-Nordheim (FN) tunneling. The larger $\Delta R/R$ at higher bias can be attributed to FN tunneling into the spin-up band of EuO—an effect that is also known to produce high P at high V in EuS barriers [21,22]. Observation of this large $\Delta R/R$ at high bias signifies that the spin-filter effect persists even at high bias, which is relevant for operating a spintronic device [23]. When even higher bias is applied, the barrier height is so low (modified by bias) that change in Φ_0 by exchange splitting does not make a significant change in tunneling probability, so that P would decrease as observed in our earlier work [21].

In conclusion, this fundamental study of the magnetic properties of high-quality, ultrathin EuO films revealed a reduction in T_C from the bulk value as thickness is reduced to a few monolayers. We have utilized the spin-filter capability of EuO barriers to quantitatively determine the amount of exchange splitting in the conduction band. Such an approach can be extended to other magnetic semiconductors and insulators. The spin-filter effect displayed here shows the potential of EuO to generate a fully spin-polarized current for spin injection.

This work at MIT was funded by NSF and ONR grants and by the KIST-MIT program. E. N., J. H., J. D., M. L., and Y. I. were supported by the ONR Grant No. N00014-03-1-0692, by the DOE under No. DE-AC06-76RL01830, and by NSF under No. DMR-0210915. The Advanced Light Source is supported by the Director, Office of Science, Office of Basic Energy Sciences, of the U.S. Department of Energy under Contract No. DE-AC02-05CH11231.

*Present address: Argonne National Laboratory, Argonne, IL, USA.

[1] P. Wachter, in *Handbook on the Physics and Chemistry of Rare Earths*, edited by K. Schneider and L. Eyring (North-Holland, New York, 1979), Vol. 2, p. 507.
[2] J. Moodera *et al.*, Phys. Rev. Lett. **61**, 637 (1988); X. Hao, J. Moodera, and R. Meservey, Phys. Rev. B **42**, 8235 (1990).
[3] J. Moodera, R. Meservey, and X. Hao, Phys. Rev. Lett. **70**, 853 (1993).
[4] T. S. Santos and J. S. Moodera, Phys. Rev. B **69**, 241203 (R) (2004).
[5] G. Busch, P. Junod, and P. Wachter, Phys. Lett. **12**, 11 (1964).
[6] W. F. Brinkman, R. C. Dynes, and J. M. Rowell, J. Appl. Phys. **41**, 1915 (1970).
[7] J. S. Moodera, T. S. Santos, and T. Nagahama, J. Phys. Condens. Matter **19**, 165202 (2007).
[8] R. Schiller and W. Nolting, Phys. Rev. Lett. **86**, 3847 (2001); R. Schiller, W. Müller, and W. Nolting, Phys. Rev. B **64**, 134409 (2001).
[9] *The Oxide Handbook*, edited by G. V. Samsonov (IFI/Plenum, New York, 1982), 2nd ed.
[10] E. Negusse, J. Holroyd, M. Liberati, J. Dvorak, Y. U. Idzerda, T. S. Santos, J. S. Moodera, and E. Arenholz, J. Appl. Phys. **99**, 08E507 (2006).
[11] J. B. Goedkoop *et al.*, Phys. Rev. B **37**, 2086 (1988).
[12] C. Wittkop, W. Schülke, and F. M. F. de Groot, Phys. Rev. B **61**, 7176 (2000).
[13] H. Ott *et al.*, Phys. Rev. B **73**, 094407 (2006).
[14] V. Chakarian, Y. U. Idzerda, and C. T. Chen, Phys. Rev. B **57**, 5312 (1998); R. Nakajima, J. Stöhr, and Y. U. Idzerda, Phys. Rev. B **59**, 6421 (1999).
[15] F. Leuenberger *et al.*, Phys. Rev. B **72**, 014427 (2005).
[16] Mg was deposited at the bottom Al/EuO interface in half of the junctions, in an effort to minimize Al_2O_3 formation, though whether Mg was present or not did not have any appreciable effect on the $R_J(T)$ behavior.
[17] J. S. Moodera and G. Mathon, J. Magn. Magn. Mater. **200**, 248 (1999).
[18] C. W. Miller *et al.*, Phys. Rev. B **74**, 212404 (2006).
[19] R. Meservey and P. M. Tedrow, Phys. Rep. **238**, 173 (1994).
[20] P. LeClair *et al.*, Appl. Phys. Lett. **80**, 625 (2002).
[21] T. Nagahama, T. S. Santos, and J. S. Moodera, Phys. Rev. Lett. **99**, 016602 (2007).
[22] A. Saffarzadeh, J. Magn. Magn. Mater. **269**, 327 (2004).
[23] S. Sugahara and M. Tanaka, Physica (Amsterdam) **21E**, 996 (2004).